Temporal Correlation of the Interference in Mobile Random Networks

Zhenhua Gong and Martin Haenggi
Department of Electrical Engineering
University of Notre Dame
Notre Dame, IN 46556, USA
{zgong, mhaenggi}@nd.edu

***Abstract*—In wireless networks, interference that is generated by undesired transmitters dominantly limits network performance. The correlation of node locations (in mobile or static networks) makes the interference temporally correlated. Such correlation affects network performance greatly, and hence needs to be quantified. In this paper, we quantify the temporal correlation of the interference in mobile Poisson networks. More specifically, we obtain closed-form expressions for the interference correlation coefficient ρ in Poisson line networks under various mobility models. When the mean speed of nodes $\bar{v}$ increases, we show that ρ is asymptotically proportional to $\bar{v}^{-1}$. Moreover, multi-path fading and random MAC schemes reduce the temporal correlation of the interference. These results are extended to higher-dimensional networks.**

***Index Terms*—Correlation, interference, mobility, Poisson point process.**

I. Introduction

In wireless networks, network performance measured by, *e.g.*, link outage, is mainly limited by interference. The characterization of the interference depends on the transmitters set, the fading and the path loss. In static networks, the distance between nodes stays constant over time, while in mobile networks, the random mobility of nodes introduces another degree of randomness in the interference characterization, *i.e.*, distance uncertainty [1].

The interference statistics of mobile networks in a single time slot has been studied in [2], by treating the network as a realization of a static model with dynamic links. However, only investigating the interference in a single time slot is insufficient to design the retransmission and routing schemes in wireless networks, since the interference is often temporally and spatially correlated. Such correlation, which is caused by the location correlation of the mobile nodes, affects retransmission and routing strategies greatly. For example in an ARQ (Automatic Repeat reQuest) retransmission mechanism, a packets is retransmitted after a timeout or after a negative acknowledgment (NACK) received. Intuitively, when the interference is correlated, so are outage events, and retransmissions do not offer the same diversity benefit as they would if outages were independent. Quantifying the correlation is hence necessary.

In [3], the spatio-temporal correlation of the interference in static networks with randomly placed nodes has been studied. To our knowledge, there is no prior work on the correlation of the interference in mobile networks. In this paper, we mainly focus on one-dimensional mobile Poisson networks. We quantify the temporal correlation of the interference in terms of the correlation coefficient under various mobility models. We then extend our results to higher dimensional networks.

II. System and Mobility Models

A. System model

At any time $t \in \mathbb{Z}$, the locations of nodes follow a Poisson point process (PPP) $\Phi(t) = \{x_i(t)\}$ on $\mathbb{R}$ of intensity λ. The Poisson model assumes the independence of the number of the nodes in disjoint regions. It is a typical mathematical model for analyzing large wireless networks. Slotted ALOHA is assumed as the MAC protocol, where each node decides to transmit independently with probability p in each time slot. We assume that every transmitter transmits with unit power.

The wireless channel is modeled by the product of a large-scale path loss component (signal attenuation over distance) and a small-scale fading component (multi-path induced). The large-scale path loss function $g(x)$ is given by

$$g(x) = \frac{1}{\epsilon + |x|^{\alpha}},$$

where $|\cdot|$ is the distance of a node to the origin, α is the path loss exponent, and $\epsilon > 0$ to keep $g(0)$ bounded. $g(x)$ is assumed to be square integrable, *i.e.*, $\int_0^\infty g^2(x)\mathrm{d}x < \infty$. For multi-path fading, we consider the Nakagami-m model with focus on the special case $m = 1$ (Rayleigh model).

B. Mobility models

The speed of a node in one time slot is defined as $v_i(t) = |x_i(t) - x_i(t-1)|$. We denote $\bar{v} = \mathbb{E}[v_i(t)]$. $\bar{v}$ is the mean speed averaged over all nodes. Due to ergodicity, the space averages are equal to the time averages.

1) Constrained i.i.d. mobility (CIM): We consider the identical CIM model defined in [1] except for one step at $t = 0$. The node location at $t+1$ is given by $x_i(t+1) = y_i + \bar{v} \cdot w_i(t)$, where the home locations of nodes $\Psi = \{y_i\}$ form a PPP, and $w_i(t)$ is a random process of location update with $\mathbb{E}[|w_i(t+1) - w_i(t)|] = 1$. We focus on the model where $w_i(t)$ is i.i.d. uniformly at random in $[-R, R]$ for $R = 1.5$. In other words, the node is mobile in an interval centered at

y_i with maximum mobility range $R\bar{v}$. When $\bar{v} \to \infty$, this model approaches the high mobility model used in [4]. The CIM model is non-Markov. However, the node locations in different time t are i.i.d. conditioned on y_i.

2) Random walk (RW): Under the RW model, each mobile node takes a step left or right with equal probability in every time slot. The speed of the node $v_i(t) \in [0, 2\bar{v}]$ is i.i.d. uniformly at random. Alternatively, the location of the node at time $t+1$ is given by $x_i(t+1) = x_i(t) + \bar{v} \cdot w_i(t)$, where $w_i(t) \in [-2, 2]$ is uniformly at random.

3) Discrete-time Brownian motion (BM): Under the discrete-time BM model, the node location at time $t+1$ is $x_i(t+1) = x_i(t) + \bar{v} \cdot w_i(t)$, where $w_i(t)$ is i.i.d. normally distributed *i.e.*, $w_i(t) \sim \mathcal{N}(0, \sigma^2)$. By definition, we have $\sigma = \sqrt{\pi/2}$.

Remark. According to [5]–[7, Lemma 2.2], the above mobility models preserve the uniform properties of the node distributions. The snapshot of a network at fixed time $t \in \mathbb{Z}$ can be viewed as a realization of a static model. Consequently for any t, the PPP $\Phi(t)$ remains homogeneous, if $\Phi(0)$ is homogeneous.

III. Temporal Correlation of Interference in Poisson Line Networks

Here we only analyze the temporal correlation of interference. Spatio-temporal correlation can be treated similarly. Because of the spatial stationarity of the point process, it is sufficient to consider the interference at the origin only. At time t, the total interference aggregated at the origin is given by

$$I(t) = \sum_{x \in \Phi(t)} T_x(t) h_x(t) g(x), \tag{1}$$

where $T_x(t)$ is i.i.d. Bernoulli with parameter p, and $h_x(t)$ is the multi-path fading gain with mean $\mathbb{E}h = 1$. $I(t)$ is identically distributed for any $t \in \mathbb{Z}$ [2]. In any snapshot, the network can be treated as static with updated node positions based on previous snapshots. We denote the temporal correlation coefficient of the interference between time s and t as $\rho_\tau \triangleq \rho_{I(t)I(s)}$, where $\tau = |t-s|$. We have the following proposition about ρ_τ.

Proposition 1. *The temporal correlation coefficient of the interferences $I(s)$ and $I(t)$, where $s \neq t$, is given by*

$$\rho_\tau = \frac{p \int_{\mathbb{R}} g(x) \mathbb{E}_{w_\tau}[g(x + \bar{v} w_\tau)] \mathrm{d}x}{\mathbb{E}[h^2] \int_{\mathbb{R}} g^2(x) \mathrm{d}x}, \tag{2}$$

where $\bar{v} w_\tau$ is the location difference of a node between time s and t.

Proof: Since $I(s)$ and $I(t)$ are identically distributed, we have

$$\rho_\tau \triangleq \frac{\mathrm{Cov}(I(t), I(s))}{\mathrm{Var}[I(t)]} = \frac{\mathbb{E}[I(t)I(s)] - \mathbb{E}[I(t)]^2}{\mathbb{E}[I(t)^2] - \mathbb{E}[I(t)]^2}, \tag{3}$$

where

$$\mu_I \triangleq \mathbb{E}[I(t)] = p\lambda \int_{\mathbb{R}} g(x) \mathrm{d}x, \tag{4}$$

and

$$\mathbb{E}[I(t)^2] = p\lambda \mathbb{E}[h^2] \int_{\mathbb{R}} g^2(x) \mathrm{d}x + p^2 \lambda^2 \left(\int_{\mathbb{R}} g(x) \mathrm{d}x \right)^2. \tag{5}$$

According to [3, (4)] and [3, (5)], (4) and (5) can be derived straightforwardly using Campbell's theorem [8]. The mean product of $I(t)$ and $I(s)$, where $t \neq s$, is given by

$$\begin{aligned}
&\mathbb{E}[I(t)I(s)] \\
&= \mathbb{E}\left[\sum_{x \in \Phi(t)} T_x(t) h_x(t) g(x) \sum_{y \in \Phi(s)} T_y(s) h_y(s) g(y) \right] \\
&= \mathbb{E}\left[\sum_{x \in \Phi(s)} T_x(t) h_x(t) g(x + \bar{v} w_\tau) \sum_{y \in \Phi(s)} T_y(s) h_y(s) g(y) \right] \\
&= \mathbb{E}\left[\sum_{x \in \Phi(s)} T_x(t) T_x(s) h_x(t) h_x(s) g(x + \bar{v} w_\tau) g(x) \right] + \\
&\quad \mathbb{E}\left[\sum_{x,y \in \Phi(s)}^{x \neq y} T_x(t) T_y(s) h_x(t) h_y(s) g(x + \bar{v} w_\tau) g(y) \right],
\end{aligned} \tag{6}$$

where $\bar{v} w_\tau$ is the location difference of a node between time s and t. Using Campbell's theorem [8], and the independence property of the multi-path fading gain h_x, we further write (6) as

$$\begin{aligned}
&\mathbb{E}[I(t)I(s)] \\
&\quad = p^2 (\mathbb{E}h)^2 \lambda \int_{\mathbb{R}} \mathbb{E}_{w_\tau}[g(x + w_\tau) g(x)] \, \mathrm{d}x \\
&\qquad + p^2 (\mathbb{E}h)^2 \lambda^2 \int_{\mathbb{R}} \int_{\mathbb{R}} \mathbb{E}_{w_\tau}[g(x + w_\tau) g(y)] \, \mathrm{d}x \mathrm{d}y \\
&\quad \overset{(a)}{=} p^2 \lambda \int_{\mathbb{R}} g(x) \mathbb{E}_{w_\tau}[g(x + w_\tau)] \, \mathrm{d}x \\
&\qquad + p^2 \lambda^2 \left(\int_{\mathbb{R}} g(x) \mathrm{d}x \right)^2,
\end{aligned} \tag{7}$$

where (a) follows from the following relationship:

$$\begin{aligned}
p\lambda \int_{\mathbb{R}} g(x) \mathrm{d}x &= \mathbb{E}[I(0)] = \mathbb{E}[I(t)] \\
&= \mathbb{E}\left[\sum_{x \in \Phi(0)} T_x(t) h_x(t) g(x + \bar{v} w_t) \right] \\
&= p\lambda \int_{\mathbb{R}} \mathbb{E}_{w_t}[g(x + \bar{v} w_t)] \mathrm{d}x
\end{aligned}$$

Therefore, (2) is proved. ∎

Examining (2), we find that its form is close to the spatio-temporal correlation coefficient in [3, (11)] for static networks. At two given locations, the spatio-temporal correlation coefficient is provided in [3, (11)], while for mobile networks, we average out the random position difference of nodes in different time slots. Furthermore, the correlation coefficient is independent of the intensity λ. With larger λ, the interference is only linearly scaled. The dependence of the interferences in two different time slots remains unchanged. Now we have the following corollary about ρ_τ.

Corollary 2. *ρ_τ is bounded by*

$$\rho_\tau \leqslant \frac{p}{\mathbb{E}[h^2]}. \tag{8}$$

Denote the pdf of w_τ as $f_{w_\tau}(z)$. If $f_{w_\tau}(0)$ is bounded, we have

$$\rho_\tau \sim C_1 \bar{v}^{-1}, \qquad \bar{v} \to \infty, \tag{9}$$

where "$\sim$" denotes asymptotic equality, and

$$C_1 = \frac{p f_{w_\tau}(0) \left(\int_{\mathbb{R}} g(x)\mathrm{d}x\right)^2}{\mathbb{E}[h^2] \int_{\mathbb{R}} g^2(x)\mathrm{d}x}.$$

If $f_{w_\tau}(0) \geqslant f_{w_\tau}(x)$, ρ_τ is bounded by

$$\rho_\tau \lesssim C_1 \bar{v}^{-1}, \qquad \bar{v} \to \infty. \tag{10}$$

Proof: Since ρ_τ decreases monotonically with $\bar{v}$, we obtain

$$\rho_\tau \leqslant \lim_{\bar{v}\to 0} \frac{p \int_{\mathbb{R}} g(x) \mathbb{E}_{w_\tau}[g(x+\bar{v}w_\tau)]\mathrm{d}x}{\mathbb{E}[h^2] \int_{\mathbb{R}} g^2(x)\mathrm{d}x} = \frac{p}{\mathbb{E}[h^2]}.$$

Exploring $\mathbb{E}_{w_\tau}[g(x+\bar{v}w_\tau)]$ in (2), we obtain

$$\begin{aligned} \mathbb{E}_{w_\tau}[g(x+\bar{v}w_\tau)] &= \int_{-\infty}^{\infty} \frac{f_{w_\tau}(z)}{\epsilon + |x+\bar{v}z|^\alpha}\mathrm{d}z \\ &= \frac{1}{\bar{v}} \int_{-\infty}^{\infty} \frac{f_{w_\tau}(t/\bar{v})}{\epsilon + |x+t|^\alpha}\mathrm{d}t. \end{aligned} \tag{11}$$

Hence when $\bar{v} \to \infty$, we have

$$\lim_{\bar{v}\to\infty} \frac{\rho_\tau}{\bar{v}^{-1}} = \frac{p f_{w_\tau}(0) \left(\int_{\mathbb{R}} g(x)\mathrm{d}x\right)^2}{\mathbb{E}[h^2] \int_{\mathbb{R}} g^2(x)\mathrm{d}x} \triangleq C_1 < \infty.$$

If $f_{w_\tau}(0) \geqslant f_{w_\tau}(x)$, $\mathbb{E}_{w_\tau}[g(x+\bar{v}w_\tau)]$ in (11) is upper bounded by

$$\mathbb{E}_{w_\tau}[g(x+\bar{v}w_\tau)] \leqslant \frac{f_{w_\tau}(0) \int_{\mathbb{R}} g(x)\mathrm{d}x}{\bar{v}}.$$

(10) is then proved. ∎

(8) is consistent to [3, Corollary 2] for static networks when $\bar{v} \to 0$. Bounded $f_{w_\tau}(0)$ indicates that the probability where a node returns to its original position after the time interval τ is equal to zero. Corollary 2 is valid for the three mobility models considered in this paper.

Interestingly, the decay of $\rho_\tau(\bar{v})$ is always asymptotically proportional to $\bar{v}^{-1}$. Figure 1 shows ρ_τ versus the mean speed $\bar{v}$ with different α under the CIM model. Figure 2 shows ρ_τ versus ϵ. When ϵ is small, ρ_τ increases with α. In this case the interferers close to the origin dominate the interference. Such dominance is more prominent with larger α and hence causes higher temporal correlation of the interference. However, ρ_τ decreases with α when ϵ is large. More nodes contribute to the interference in this case. The slower the path loss decays, the more correlated the interference is.

The integral $\int_{\mathbb{R}} g(x)\mathbb{E}_{w_\tau}[g(x+\bar{v}w_\tau)]\mathrm{d}x$ in (2) depends on the mobility model. In the next several subsections, we discuss different mobility models individually.

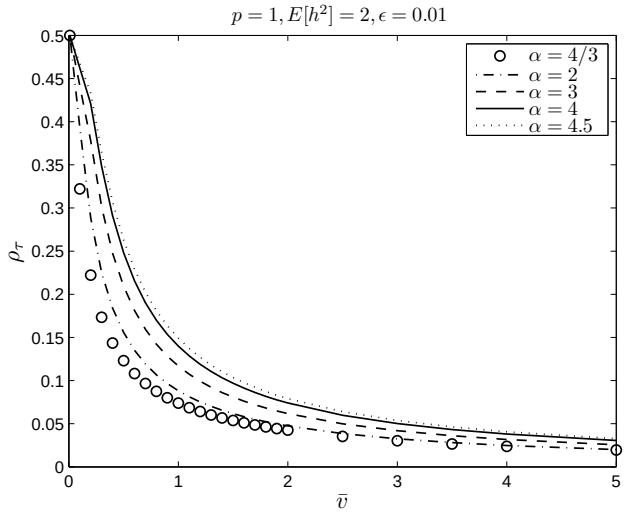

Figure 1. The temporal correlation coefficient ρ_τ versus the mean speed $\bar{v}$ with different path loss exponent α for the CIM model.

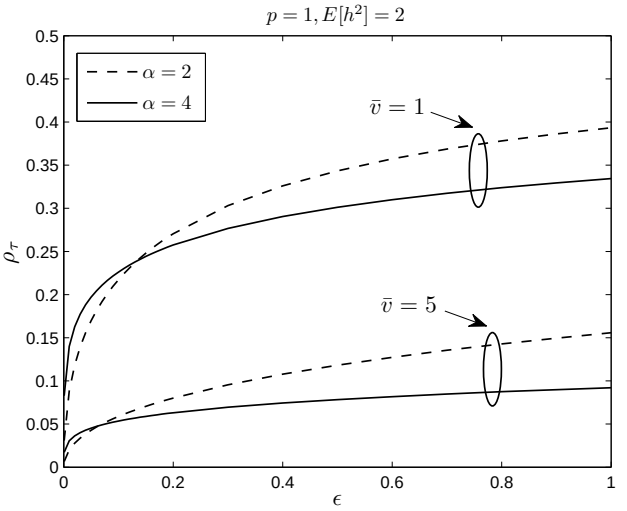

Figure 2. The temporal correlation coefficient ρ_τ versus ϵ for the CIM model.

A. Constrained i.i.d. mobility (CIM)

Under the CIM model, the first term in (6) can be rewritten as

$$\begin{aligned} &\mathbb{E}\left[\sum_{x\in\Phi(s)} T_x(t)T_x(s)h_x(t)h_x(s)g(x+\bar{v}w_\tau)g(x)\right] \\ &\quad \overset{(a)}{=} p^2\mathbb{E}\left[\sum_{x\in\Psi} g(x+\bar{v}w_t)g(x+\bar{v}w_s)\right] \\ &\quad \overset{(b)}{=} p^2\lambda \int_{\mathbb{R}} \mathbb{E}_{w_s}[g(x+\bar{v}w_s)]^2\mathrm{d}x, \end{aligned}$$

where (a) follows from the independence of $T_x(t)$ and $T_x(s)$; (b) follows from the fact that $w_t, w_s \in [-1.5, 1.5]$ are i.i.d.

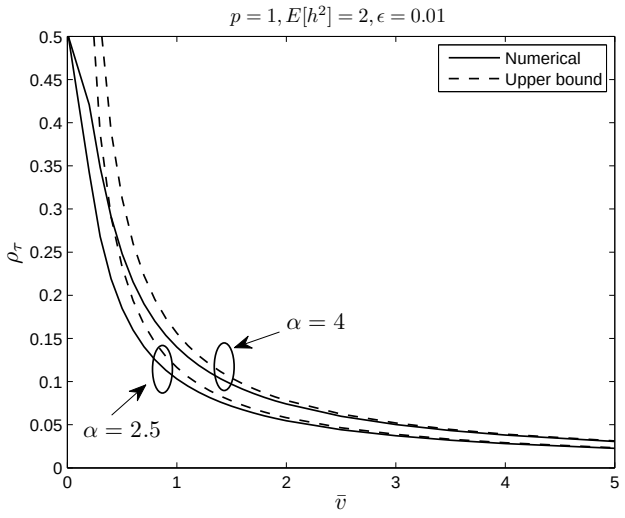

Figure 3. Numerical evaluation (from (12)) of the temporal correlation coefficient ρ_τ versus $\bar{v}$ with the corresponding approximation (from (13)). The mobility model is CIM.

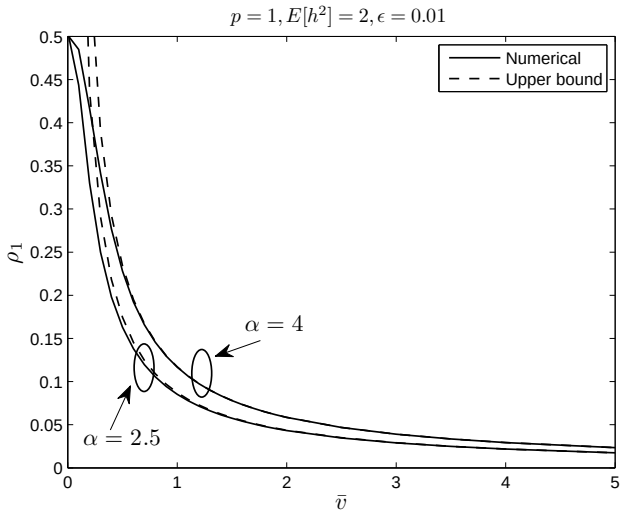

Figure 4. Numerical evaluation (from (2)) of the temporal correlation coefficient ρ_1 versus $\bar{v}$ with the corresponding approximation (from (14)). The mobility model is RW.

and uniformly at random. Thus, $\rho_{\tau,\mathrm{CIM}}$ is given by

$$\rho_{\tau,\mathrm{CIM}} = \frac{p\int_{\mathbb{R}} \mathbb{E}_{w_s}[g(x+\bar{v}w_s)]^2 \mathrm{d}x}{\mathbb{E}[h^2]\int_{\mathbb{R}} g^2(x)\mathrm{d}x}. \tag{12}$$

Using the limit in (10) as an approximation, we have the following corollary about $\rho_{\tau,\mathrm{CIM}}$.

Corollary 3. *$\rho_{\tau,\mathrm{CIM}}$ can be upper bounded by*

$$\rho_{\tau,\mathrm{CIM}} \lessapprox \frac{p}{\mathbb{E}[h^2]} \cdot \min\left\{1, \frac{2\pi\epsilon^{1/\alpha}}{3(\alpha-1)\sin(\pi/\alpha)\bar{v}}\right\}. \tag{13}$$

Proof: Since we have

$$\int_{\mathbb{R}} g(x)\mathrm{d}x = \frac{2\pi}{\alpha\epsilon^{1-1/\alpha}\sin(\pi/\alpha)},$$

and

$$\int_{\mathbb{R}} g^2(x)\mathrm{d}x = \frac{2(\alpha-1)\pi}{\alpha^2\epsilon^{2-1/\alpha}\sin(\pi/\alpha)},$$

(13) then follows from Corollary 2 after several steps of calculation. ∎

Figure 3 shows the numerical evaluation of $\rho_{\tau,\mathrm{CIM}}$ from (12) (solid-line curves) together with the approximation from (13) (dash-line curves). The approximation converges to the numerical evaluation fast as $\bar{v}$ increases, and thus provides a tight approximation for all $\alpha > 1$.

From (12) and (13), we find that the temporal correlation remains stationary over time under the CIM model, since $\rho_{\tau,\mathrm{CIM}}$ is independent of τ. This observation matches with the property of the CIM model. For the Nakagami-m fading model, we have $\mathbb{E}[h^2] = \frac{m+1}{m}$. In particular, $\mathbb{E}[h^2] = 2$ for Rayleigh fading ($m = 1$), and $\mathbb{E}[h^2] = 1$ for no fading ($m \to \infty$). $\rho_{\tau,\mathrm{CIM}}$ increases with m. So as with the MAC scheme parameter p. Alternatively, both fading and random MAC scheduling schemes reduce the temporal correlation of interference.

B. Random walk (RW)

Under the RW model, we focus on the temporal correlation of the interference between two successive time slots *i.e.*, ρ_1. By a similar derivation as for the CIM model, we have the following corollary about $\rho_{1,\mathrm{RW}}$.

Corollary 4. *The upper bound of $\rho_{1,\mathrm{RW}}$ is given by*

$$\rho_{1,\mathrm{RW}} \lessapprox \frac{p}{\mathbb{E}[h^2]} \cdot \min\left\{1, \frac{\pi\epsilon^{1/\alpha}}{2(\alpha-1)\sin(\pi/\alpha)\bar{v}}\right\}. \tag{14}$$

Figure 4 displays the numerical evaluation of $\rho_{1,\mathrm{RW}}$ from (2) and its approximation from (14). Straightforwardly, the approximation converges fast to the numerical evaluation.

When $\tau > 1$, we have $w_\tau = \sum_{i=1}^{\tau} w(i)$, where $w(i) \in [-2, 2]$ is i.i.d. uniformly at random. Hence, the pdf of w_τ is given by

$$f_{w_\tau}(z) = \frac{1}{2\pi}\int_{-\infty}^{\infty}\left(\frac{\sin(2\bar{v}\omega)}{2\bar{v}\omega}\right)^{\tau} e^{-j\omega z}\mathrm{d}\omega.$$

It is hard to get a closed-form $\rho_{\tau,\mathrm{RW}}$ expression for $\tau > 1$. However, numerical evaluation can be obtained, which is shown in Figure 6.

C. Discrete-time Brownian motion (BM)

Under the BM model, we have $w_\tau = \sum_{i=1}^{\tau} w(i) = \sqrt{\tau}w_0$, where w_0 is a normal random variable, *i.e.*, $\mathcal{N}(0, \sigma^2)$. Hence, (2) can be rewritten as

$$\rho_{\tau,\mathrm{BM}} = \frac{p\int_{\mathbb{R}} g(x)\,\mathbb{E}_{w_0}[g(x+\sqrt{\tau}\bar{v}w_0)]\,\mathrm{d}x}{\mathbb{E}[h^2]\int_{\mathbb{R}} g^2(x)\mathrm{d}x}. \tag{15}$$

Figure 5 plots ρ_1 versus the mean speed of nodes $\bar{v}$ under three mobility models. As we observe from the figure, $\rho_{1,\mathrm{CIM}}$ and $\rho_{1,\mathrm{BM}}$ are approximately equal. $\rho_{1,\mathrm{RW}}$ decays slightly faster with the increase of $\bar{v}$. The discrepancy between them is less than 0.02. The mean speed $\bar{v}$ rather than the mobility models themselves affects the temporal correlation of interference

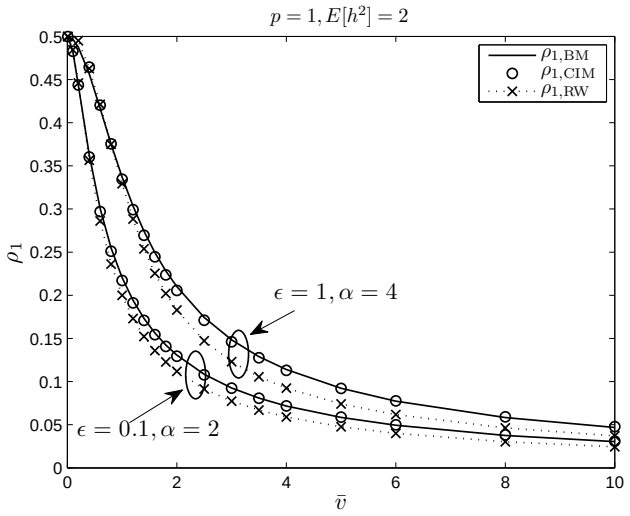

Figure 5. The interference correlation coefficient ρ_1 versus the mean speed $\bar{v}$ under three mobility models.

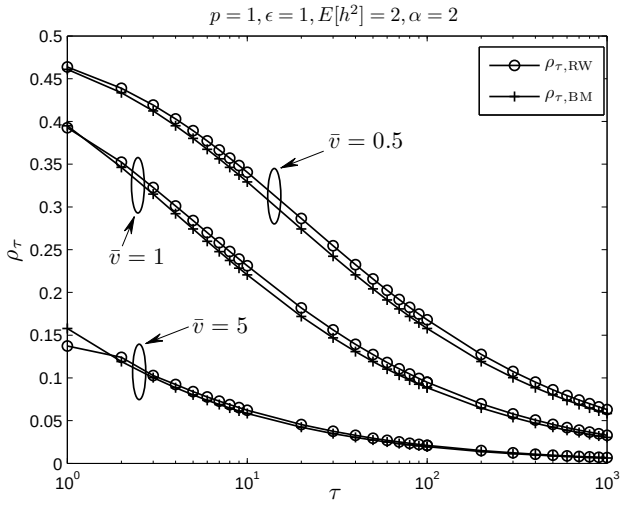

Figure 6. The interference correlation coefficient ρ_τ versus the time difference τ under the RW and BM models. $\rho_{\tau,\mathrm{CIM}}$ is constant over τ and its value can be read from Figure 5.

greatly. For $\tau > 1$, we have the following corollary about $\rho_{\tau,\mathrm{BM}}$.

Corollary 5. *When $\tau \to \infty$, we have*

$$\rho_{\tau,\mathrm{BM}} \sim C_2 \tau^{-1/2}, \tag{16}$$

where

$$C_2 = \frac{C_1}{\bar{v}} = \frac{2\epsilon^{1/\alpha}}{(\alpha-1)\sin(\pi/\alpha)\bar{v}},$$

and $\rho_{\tau,\mathrm{BM}}$ is bounded by

$$\rho_{\tau,\mathrm{BM}} \lessapprox \frac{p}{\mathbb{E}[h^2]} \cdot \min\left\{1, \frac{2\epsilon^{1/\alpha}}{(\alpha-1)\sin(\pi/\alpha)\sqrt{\tau}\bar{v}}\right\}. \tag{17}$$

Proof: Based on Corollary 2, (16) and (17) follow from (15) after a few elementary steps. ∎

Figure 6 shows the decay of ρ_τ versus τ. $\rho_{\tau,\mathrm{BM}}$ decays slightly faster than $\rho_{\tau,\mathrm{RW}}$. $\rho_{\tau,\mathrm{CIM}}$ is constant over τ and its value can be read from Figure 5.

IV. Temporal Correlation of Interference in Higher-Dimensional Networks

In d-dimensional networks, the path loss function $g(x)$ is given by

$$g(x) = \frac{1}{\epsilon + \|x\|^\alpha},$$

where $\|\cdot\|$ is the Euclidean distance. Hence by a similar derivation as in Proposition 1, ρ_τ is given by

$$\rho_\tau = \frac{p \int_{\mathbb{R}^d} g(x)\mathbb{E}_{w_\tau}[g(x+\bar{v}w_\tau)]\,\mathrm{d}x}{\mathbb{E}[h^2]\int_{\mathbb{R}^d} g^2(x)\mathrm{d}x}. \tag{18}$$

V. Conclusions

In this paper, we have quantified the temporal correlation of the interference in mobile networks in terms of the correlation coefficient ρ. We have shown that ρ decreases asymptotically inversely proportionally with the mean speed of nodes. Multi-path fading and random MAC schemes also reduce the interference correlation. The interference correlation coefficient is a key ingredient when exploring the outage correlation in wireless networks.

Acknowledgments

The partial support of NSF (grants CNS 04-47869, CCF 728763) and the DARPA/IPTO IT-MANET program (grant W911NF-07-1-0028) is gratefully acknowledged.

References

[1] Z. Kong and E. Yeh, "On the latency for information dissemination in mobile wireless networks," in *Proceedings of the 9th ACM International Symposium on Mobile Ad Hoc Networking and Computing (MobiHoc)*, Hong Kong SAR, China, May 2008.

[2] Z. Gong and M. Haenggi, "Mobility and fading: Two sides of the same coin," in *2010 IEEE Global Communications Conference (GLOBECOM'10)*, (Miami, FL), 2010.

[3] R. Ganti and M. Haenggi, "Spatial and temporal correlation of the interference in ALOHA ad hoc networks," *IEEE Communications Letters*, vol. 13, no. 9, pp. 631–633, 2009.

[4] M. Grossglauser and D. Tse, "Mobility increases the capacity of ad hoc wireless networks," *IEEE/ACM Transactions on Networking (ToN)*, vol. 10, no. 4, pp. 477–486, 2002.

[5] P. Nain, D. Towsley, B. Liu, Z. Liu, and F. Inria, "Properties of random direction models," in *Proceedings IEEE INFOCOM 2005. 24th Annual Joint Conference of the IEEE Computer and Communications Societies*, vol. 3, 2005.

[6] F. Baccelli, B. Blaszczyszyn, and P. Muhlethaler, "An Aloha protocol for multihop mobile wireless networks," *IEEE Transactions on Information Theory*, vol. 52, no. 2, pp. 421–436, 2006.

[7] S. Bandyopadhyay, E. J. Coyle, and T. Falck, "Stochastic properties of mobility models in mobile ad hoc networks," *IEEE Transactions on Mobile Computing*, vol. 6, no. 11, pp. 1218–1229, 2007.

[8] D. Stoyan, W. Kendall, and J. Mecke, *Stochastic geometry and its applications*. Wiley Chichester, 1995.